

DOI:10.1002/ejic.201402326

# Tetranuclear [2×2] Square-Grid Lanthanide(III) Complexes: Syntheses, Structures, and Magnetic Properties

Sourav Biswas,<sup>[a]</sup> Sourav Das,<sup>[a]</sup> Jan van Leusen,<sup>[b]</sup> Paul Kögerler,<sup>\*[b]</sup> and Vadapalli Chandrasekhar<sup>\*[a,c]</sup>

**Keywords:** Lanthanides / Cluster compounds / Schiff bases / Magnetic properties

The reactions of lanthanide(III) nitrate salts (Dy<sup>III</sup>, Tb<sup>III</sup>, Gd<sup>III</sup>, and Er<sup>III</sup>) with the aroylhydrazone-based multidentate ligand 6-(hydroxymethyl)-*N'*-[1-(pyridin-2-yl)ethylidene]picolinohydrazide (LH<sub>2</sub>) in the presence of Et<sub>3</sub>N in a molar ratio of 1:1:4 afforded a series of homometallic tetranuclear lanthanide(III) complexes, [Ln<sub>4</sub>(LH)<sub>4</sub>(μ<sub>2</sub>-OH)<sub>3</sub>(μ<sub>2</sub>-OMe)]<sub>4</sub>NO<sub>3</sub>·*x*MeOH·*y*H<sub>2</sub>O (**1**, Ln = Dy, *x* = 2, *y* = 4; **2**, Ln = Tb, *x* = 2, *y* = 4; **3**, Ln = Gd, *x* = 2, *y* = 5; and **4**, Ln = Er, *x* = 3, *y* = 3). X-ray diffraction studies revealed that all of the complexes contain a tetracationic [2×2] square-grid-like [Ln<sub>4</sub>(μ<sub>2</sub>-OH)<sub>3</sub>(μ<sub>2</sub>-OMe)(μ<sub>2</sub>-O)<sub>4</sub>]<sup>4+</sup> core, which is assembled by the concerted coordi-

nation action of four monoanionic [LH]<sup>-</sup> ligands along with three μ<sub>2</sub>-OH ligands and a μ<sub>2</sub>-OMe ligand. All of the lanthanide centers are eight-coordinate and adopt distorted triangular-dodecahedral coordination geometries with two different types of coordination environments (6O,2N and 4O,4N). The magnetic susceptibility measurements of the complexes reveal both the presence of all-antiferromagnetic coupling interactions as well as both isotropic (**3**) and anisotropic (**1**, **2**, **4**) single-ion contributions, which do not result in slow relaxation characteristics typical of single-molecule magnets.

## Introduction

Polynuclear lanthanide(III) complexes are increasingly studied for a variety of reasons including their applications in catalysis,<sup>[1]</sup> luminescence,<sup>[2]</sup> molecular magnetism,<sup>[3]</sup> and biological imaging.<sup>[4]</sup> Various types of ligands have been employed to assemble such polynuclear compounds, the nuclearity of which can be varied from 1 to 60.<sup>[5]</sup> Among such compounds, the tetranuclear complexes possess large structural diversity (Table S1, Supporting Information). Despite the significant amount of structural diversity that the tetranuclear analogues possess, only three examples are known in which the lanthanide ions are arranged in a planar square-type geometry.<sup>[6–8]</sup> On the other hand, we have recently reported a planar rhombus-shaped tetranuclear ensemble (Scheme 1, a).<sup>[9]</sup>

To understand the formation of planar tetranuclear lanthanide arrays with grid-type geometry, we have now designed a new aroylhydrazone-based Schiff base ligand, 6-(hydroxymethyl)-*N'*-[1-(pyridin-2-yl)ethylidene]picolinohydrazide (LH<sub>2</sub>). The reaction of LH<sub>2</sub> with Ln(NO<sub>3</sub>)<sub>3</sub>·*x*H<sub>2</sub>O (Ln = Dy, Tb, Gd, and Er; *x* = 5 for Dy, Tb, Er and *x* = 6 for Gd) afforded the tetranuclear [2×2] square-grid complexes **1–4**, [Ln<sub>4</sub>(LH)<sub>4</sub>(μ<sub>2</sub>-OH)<sub>3</sub>(μ<sub>2</sub>-OMe)]<sub>4</sub>NO<sub>3</sub>·*x*MeOH·*y*H<sub>2</sub>O (Dy, *x* = 2, *y* = 4; Tb, *x* = 2, *y* = 4; Gd, *x* = 2, *y* = 5; and Er, *x* = 3, *y* = 3). The synthesis, structure, and magnetism of these complexes are discussed herein.

## Results and Discussion

### Synthesis and Structural Characterization

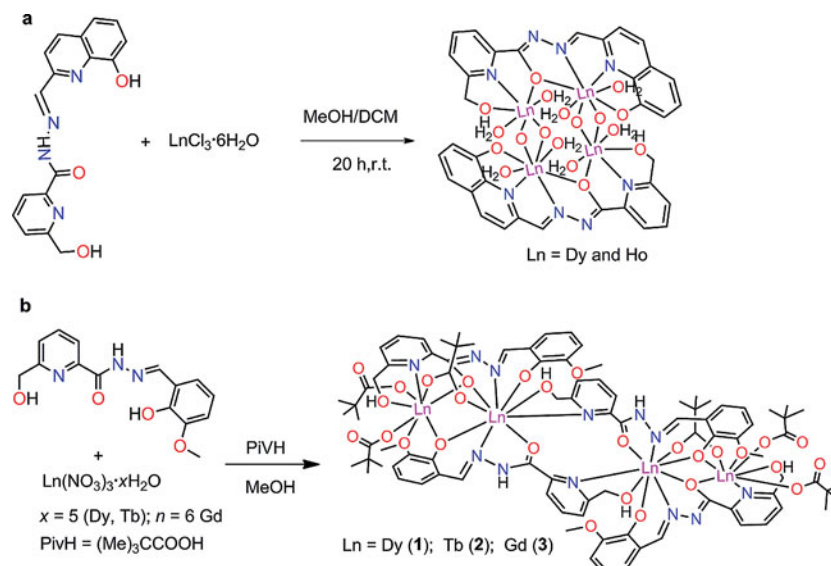
A survey of the recent literature reveals that the employment of multidentate Schiff base ligands is a very promising method for obtaining multinuclear homometallic 4f complexes. Among these, aroylhydrazone-based Schiff base ligands are attractive because of their keto–enol tautomerization, which provides an additional feature for the formation of polynuclear aggregates. We have previously utilized such a ligand to afford a tetranuclear complex containing two dinuclear subunits (Scheme 1, b).<sup>[10]</sup> In the current study, we have employed a multisite coordinating compartmental Schiff base ligand, (*E*)-6-(hydroxymethyl)-*N'*-

[a] Department of Chemistry, Indian Institute of Technology Kanpur, Kanpur 208016, India  
E-mail: vc@iitk.ac.in  
<http://www.iitk.ac.in>

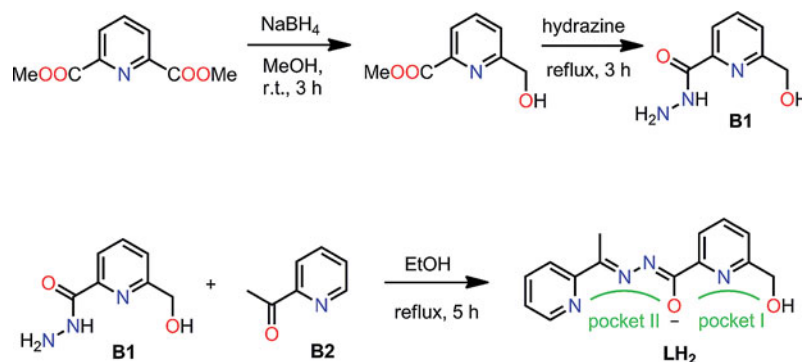
[b] Institut für Anorganische Chemie, RWTH Aachen University, 52074 Aachen, Germany  
E-mail: paul.koegerler@ac.rwth-aachen.de  
<http://www.ac.rwth-aachen.de>

[c] National Institute of Science Education and Research, Institute of Physics Campus, Sachivalaya Marg, PO: Sainik School, Bhubaneswar 751005, India  
<http://www.niser.ac.in>

Supporting information for this article is available on the WWW under <http://dx.doi.org/10.1002/ejic.201402326>.



Scheme 1. Synthesis of (a) rhombus-shaped tetranuclear lanthanide complexes<sup>[9]</sup> and (b) Ln<sub>4</sub> complexes containing two dinuclear subunits.<sup>[10]</sup>



Scheme 2. Synthesis of LH<sub>2</sub>. The coordination pockets are indicated.

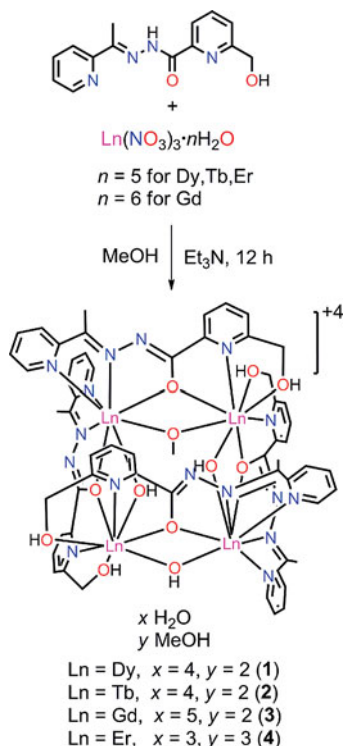
[1-(pyridin-2-yl)ethylidene]picolinohydrazide (LH<sub>2</sub>). It was prepared by two-step synthetic protocol, in which the first step involves the preparation of 6-(hydroxymethyl)picolinohydrazide (**B1**), which undergoes a Schiff base condensation reaction with 2-acetylpyridine (**B2**) to afford LH<sub>2</sub> (Scheme 2).

The ligand LH<sub>2</sub> has six potential coordination sites with two distinct compartments; one of these possesses a pendant –CH<sub>2</sub>OH arm, a pyridine nitrogen atom, and a common bridging enolate oxygen atom (chelating ONO donor). The other compartment consists of the common bridging enolate oxygen atom, an imino nitrogen atom, and a pyridine nitrogen atom (tridentate ONN donor; Scheme 2). The sequential reaction of LH<sub>2</sub> with lanthanide salts in the presence of triethylamine in a 1:1:4 stoichiometric ratio afforded the homometallic [2×2] square-grid lanthanide complexes [Ln<sub>4</sub>(LH)<sub>4</sub>(μ<sub>2</sub>-OH)<sub>3</sub>(μ<sub>2</sub>-OMe)]4NO<sub>3</sub>·xMeOH·yH<sub>2</sub>O (**1**: Dy, x = 2, y = 4; **2**: Tb, x = 2, y = 4; **3**: Gd, x = 2, y = 5; and **4**: Er, x = 3, y = 3) in excellent yields (≥60%, Scheme 3; see Experimental Section).

## X-ray Crystal Structures of 1–4

Single-crystal X-ray analysis revealed that **1–4** crystallize in the monoclinic system in the space group *P2<sub>1</sub>/n* with *Z* = 4. All of the complexes are tetracationic in nature and contain four nitrate anions to balance the charge. Owing to the structural similarity of **1–4**, only the structure of **2** is described in detail here. The molecular structure of **2** is shown in Figure 1a, and those of **1**, **3**, and **4** are given in the Supporting Information (Figures S1–S3). Selected bond parameters of **2** are summarized in the Table 1. The other bond parameters including those of **1**, **3**, and **4** are listed in the Supporting Information (Tables S2–S4).

The molecular structure of **2** reveals that the four Tb<sup>III</sup> ions are tightly held together by four heptadentate monodeprotonated [LH]<sup>−</sup> Schiff base ligands. Each ligand binds to two Tb<sup>III</sup> ions through the two tridentate NNO and NOO pockets with further assistance from the bridging enolizable hydrazone oxygen atom. In addition, **2** contains three μ-OH ligands and one μ-OMe ligand (Figure 1, b). Interestingly,



Scheme 3. Synthesis of tetranuclear  $[2 \times 2]$  square-grid lanthanide(III) complexes **1–4**.

the formation of **2** involves exclusively the enol form of the ligand  $[\text{LH}]^-$ . This may be contrasted with the situation in the  $\text{Ln}_4$  complexes in Scheme 1 (b), in which both the keto and the enol forms of  $N'$ -(2-hydroxy-3-methoxybenzylidene)-6-(hydroxymethyl)picolinohydrazide are used.

The tetracationic  $[\text{Tb}_4(\mu_2\text{-OH})_3(\mu_2\text{-OMe})(\mu_2\text{-O})_4]^{4+}$  core of the complex possesses an almost  $[2 \times 2]$  square-grid topology. As mentioned above, only three such examples were known previously.<sup>[7,17,18]</sup> The overall structure of **2** contains two distinct eight-coordinate  $\text{Tb}^{\text{III}}$  ions; one of them contains a  $6\text{O}, 2\text{N}$  coordination environment, whereas the other possesses a  $4\text{O}, 4\text{N}$  coordination environment (Figure 2). The Tb–N distances of the two different types of coordina-

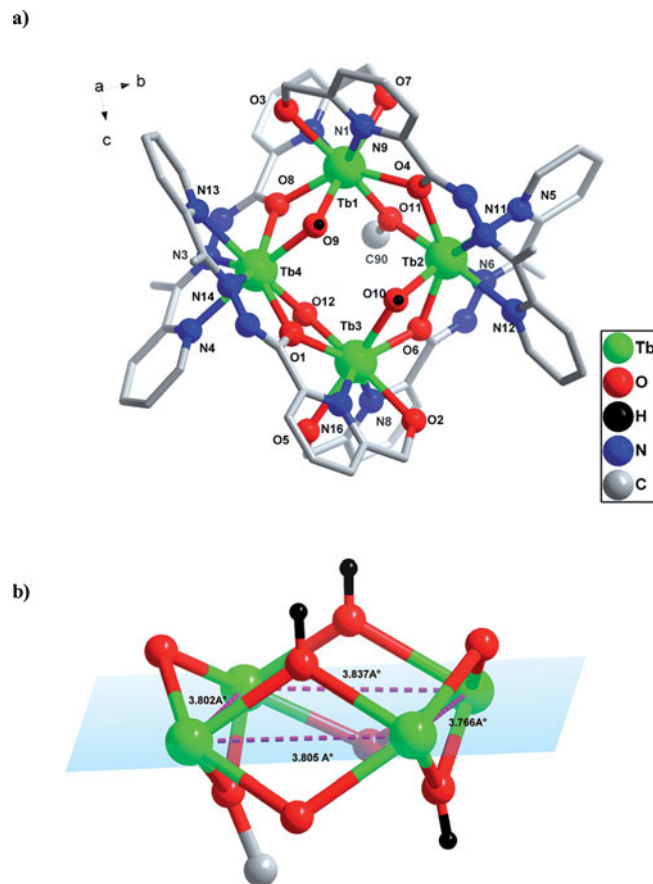


Figure 1. (a) Molecular structure of **2** (hydrogen atoms, the solvent molecules, and all nitrate anions have been omitted for clarity). (b) The  $[2 \times 2]$  square core of **2**.

tion centers are very similar and are in the range ca. 2.517–2.568 Å. The Tb–O bond lengths vary depending upon the nature of the oxygen atom: the range ca. 2.326–2.414 Å corresponds to the Tb– $\text{O}_{\text{enolate}}$  bonds, whereas the range 2.264–2.321 Å corresponds to the Tb– $\text{OH}_{\text{bridging}}$  bonds. An inspection of the Tb–Tb distances reveals that there is a slight deviation from a perfect square geometry.

Table 1. Selected bond lengths [Å] and angles [°] for **2**.

| Bond        | Length   | Bond        | Length   | Bonds             | Angle      |
|-------------|----------|-------------|----------|-------------------|------------|
| Tb(1)–O(3)  | 2.400(5) | Tb(3)–O(2)  | 2.407(5) | Tb(2)–O(11)–Tb(1) | 111.33(18) |
| Tb(1)–O(4)  | 2.372(4) | Tb(3)–O(12) | 2.276(5) | Tb(2)–O(10)–Tb(3) | 112.5(2)   |
| Tb(1)–O(7)  | 2.410(5) | Tb(3)–O(5)  | 2.413(5) | Tb(4)–O(12)–Tb(3) | 112.1(2)   |
| Tb(1)–O(8)  | 2.346(5) | Tb(3)–O(6)  | 2.362(5) | Tb(4)–O(9)–Tb(1)  | 113.9(2)   |
| Tb(1)–O(9)  | 2.277(5) | Tb(3)–O(10) | 2.320(5) | Tb(4)–O(8)–Tb(1)  | 108.48(18) |
| Tb(1)–N(1)  | 2.550(6) | Tb(3)–O(1)  | 2.346(5) | Tb(4)–O(1)–Tb(3)  | 107.43(19) |
| Tb(1)–N(9)  | 2.529(6) | Tb(3)–N(8)  | 2.517(6) | Tb(2)–O(6)–Tb(3)  | 109.69(18) |
| Tb(2)–O(4)  | 2.352(4) | Tb(3)–N(16) | 2.538(6) | Tb(2)–O(4)–Tb(1)  | 107.19(17) |
| Tb(2)–O(6)  | 2.331(5) | Tb(4)–O(8)  | 2.343(4) |                   |            |
| Tb(2)–O(10) | 2.294(5) | Tb(4)–O(9)  | 2.263(5) |                   |            |
| Tb(2)–O(11) | 2.298(4) | Tb(4)–O(12) | 2.265(5) |                   |            |
| Tb(2)–N(5)  | 2.569(6) | Tb(4)–O(1)  | 2.327(4) |                   |            |
| Tb(2)–N(6)  | 2.521(6) | Tb(4)–N(3)  | 2.537(6) |                   |            |
| Tb(2)–N(11) | 2.518(6) | Tb(4)–N(4)  | 2.562(6) |                   |            |
| Tb(2)–N(12) | 2.541(6) | Tb(4)–N(13) | 2.567(6) |                   |            |
|             |          | Tb(4)–N(14) | 2.564(6) |                   |            |

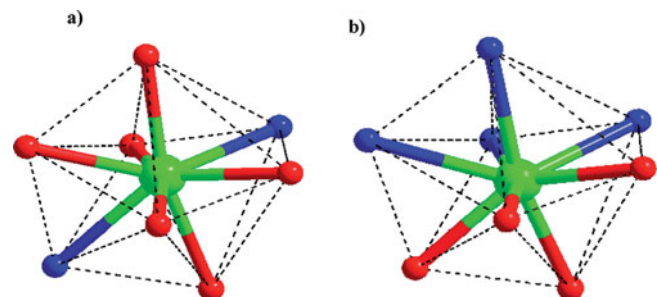


Figure 2. (a) Distorted triangular-dodecahedral geometries around (a) the  $\text{Tb}^{3+}$  ion with a 6O,2N coordination environment and (b) the  $\text{Tb}^{3+}$  ion with a 4O,4N coordination environment.

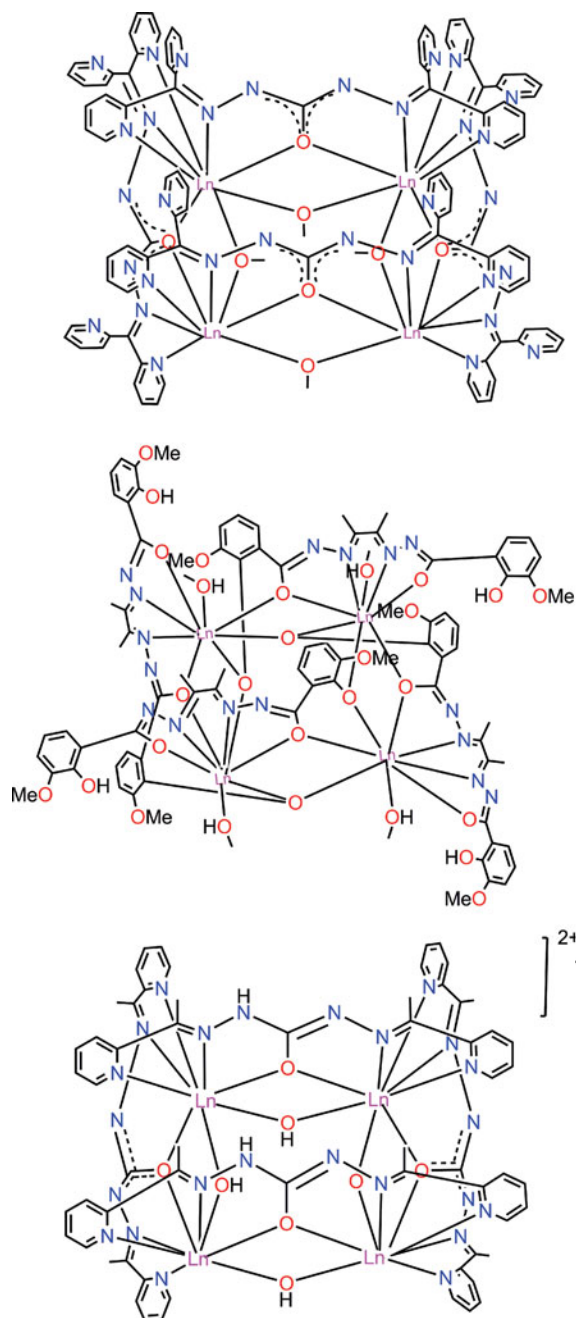


Figure 3. Previously reported tetranuclear  $[2 \times 2]$  square-grid complexes.<sup>[6–8]</sup>

As mentioned above, three tetranuclear square-grid lanthanide complexes with aroylhydrazone-based ligands have been reported previously (Figure 3). The metric parameters in these complexes are quite similar to those in the present instance, in spite of the differences in their structural features (Table 2).

Table 2. Comparison of the bond lengths [Å] and angles [°] of tetranuclear complexes with a  $[2 \times 2]$  square-grid structure.

|   | Ln–N <sub>py</sub> | Ln–N <sub>imino</sub> | Ln–Ln     | Ln–O–Ln       | Ref.      |
|---|--------------------|-----------------------|-----------|---------------|-----------|
| $[\text{Ln}_4(\text{L}_1)_4(\text{Cl}_1)_4]$                                  |                    |                       |           |               |           |
| $\text{L1}_1 =$   | 2.53–2.56          | 2.53–2.57             | 3.77–3.78 | 108.47–109.11 | 7         |
| $[\text{Ln}_4(\text{HL}_3)_4(\text{MeOH})_4]$                                 |                    |                       |           |               |           |
| $\text{L1}_3 =$   |                    | 2.45–2.49             | 3.82–3.87 | 107.26–109.94 | 6         |
| $[\text{Ln}_4(\text{L}_2)_4(\text{OH})_4]\text{Cl}_2$                         |                    |                       |           |               |           |
| $\text{LH}_2 =$   | 2.540–2.56         | 2.52–2.53             | 3.76–3.79 | 107.38–108.44 | 8         |
| $\text{Ln}_4(\text{L1})_4(\mu_2\text{-OH})_4(\mu_2\text{-OMe})_4\text{HNO}_3$ |                    |                       |           |               |           |
| $\text{L1}_2 =$   | 2.48–2.576         | 2.47–2.59             | 3.78–3.82 | 107.20–110.80 | this work |

## Magnetic Properties

The computational framework CONDON<sup>[11]</sup> has been used in the analysis of the magnetochemical data of **1–4**. The simulations account for all of the microscopic aspects necessary to model the 4f electronic structure, in particular the relevant single-ion effects and coupling interactions. In addition, ligand-field effects, spin–orbit coupling, and the external magnetic field have been considered. Standard values were employed for spectroscopic parameters such as the Slater–Condon parameters  $F^2$ ,  $F^4$ , and  $F^6$  and the single-electron spin–orbit coupling energies  $\zeta_{4f}$ . Alternatively, CONDON implements an effective isotropic spin model, which was used for **3** ( $\text{Gd}^{\text{III}}$ ).

The magnetic properties of **1–4** are primarily characterized by the single-ion effects and exchange interactions of the lanthanide ions that form the  $[2 \times 2]$  square core (Figure 1). The single-ion effects of the lanthanides were determined by electron–electron repulsions, spin–orbit coupling, and ligand-field effects (magnitude of interactions in decreasing order). These remove the degeneracy of the ground states of the free ions [**1**:  $\text{Dy}^{\text{III}}$  ( $^6\text{H}_{15/2}$ ), **2**:  $\text{Tb}^{\text{III}}$  ( $^7\text{F}_6$ ), **3**:  $\text{Gd}^{\text{III}}$  ( $^8\text{S}_{7/2}$ ), and **4**:  $\text{Er}^{\text{III}}$  ( $^4\text{I}_{15/2}$ )].

Owing to the simple nature of the magnetism of  $\text{Gd}^{\text{III}}$  compounds and to develop a general understanding of the exchange interaction pathways in **1–4**, compound **3** was analyzed first. The magnetic susceptibility of **3** was measured at three different applied magnetic fields (0.1, 3, and 5 T; Figure 3). The  $\chi_{\text{M}}T$  value of  $30.9 \text{ cm}^3 \text{ K mol}^{-1}$  at 290 K is in the range commonly expected for four noninteracting  $\text{Gd}^{\text{III}}$  centers ( $30.4\text{--}31.2 \text{ cm}^3 \text{ K mol}^{-1}$ ).<sup>[12]</sup> As the temperature de-

creases, the  $\chi_M T$  value continuously decreases, which indicates that there are saturation effects in the single-ion contribution and/or dominant antiferromagnetic coupling of the Gd<sup>III</sup> centers.

The data of **3** were modeled by an effective isotropic spin Hamiltonian that describes a system of isotropic  $S = 7/2$  centers. Further analysis showed that three different exchange interaction pathways are sufficient to describe the magnetic susceptibility data in **3**. They are directly related to the Gd<sup>III</sup>–Gd<sup>III</sup> distances in the slightly distorted [2×2] square core (Figure 4):  $|J_1|$  (shortest) >  $|J_2|$  (×2, medium) >  $|J_3|$  (largest distance). Thus, the exchange interaction Hamiltonian is:

$$\hat{H}_{\text{ex}} = -2J_1\hat{H}_{\text{Gd1}}\cdot\hat{H}_{\text{Gd2}} - 2J_2(\hat{H}_{\text{Gd2}}\cdot\hat{H}_{\text{Gd3}} + \hat{H}_{\text{Gd3}}\cdot\hat{H}_{\text{Gd4}}) - 2J_3\hat{H}_{\text{Gd4}}\cdot\hat{H}_{\text{Gd1}}$$

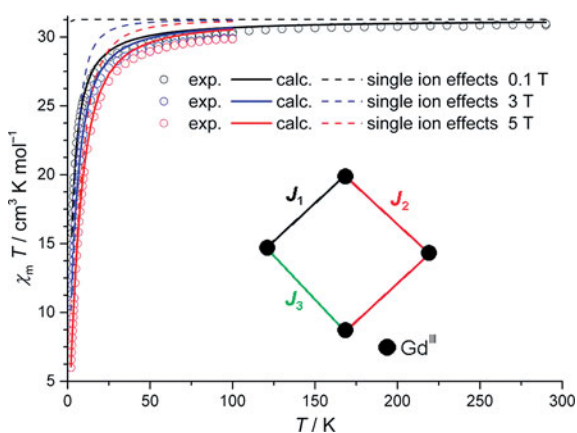


Figure 4. Temperature dependence of  $\chi_M T$  of **3** at different applied magnetic fields. The single-ion effects of four noninteracting Gd<sup>III</sup> centers are shown for comparison. Inset: coupling scheme.

The result of the corresponding fit is depicted in Figure 4 (solid lines) for an effective  $g$  value of  $g_{\text{eff}} = 1.9925$  (quality-of-fit parameter  $\text{SQ} = 1.5\%$  including field dependence of the magnetization at 2 K, not shown). To distinguish exchange interaction contributions from single-ion effects, the simulated curves with the exchange interactions omitted are shown as dashed lines.

The least-squares fit reveals that all of the exchange interactions are antiferromagnetic, which results in a singlet ground state for the [2×2] square Gd<sub>4</sub> core. The exchange interaction parameters  $J_1 = -0.11 \text{ cm}^{-1}$ ,  $J_2 = -0.06 \text{ cm}^{-1}$ , and  $J_3 = -0.03 \text{ cm}^{-1}$  are within the range expected for (weakly) interacting lanthanide ions ( $|J| \leq 1 \text{ cm}^{-1}$ ).<sup>[13]</sup>

For **1**, **2**, and **4**, the  $\chi_M T$  values of 55.0 (**1**), 46.6 (**2**), and 44.1  $\text{cm}^3 \text{K mol}^{-1}$  (**4**) at 290 K (Figure 5) are in or slightly lower than the intervals expected for the four corresponding, noninteracting Ln<sup>III</sup> centers [52.0–56.2 (Dy<sup>III</sup>), 47.1–48.0 (Tb<sup>III</sup>), and 44.2–45.1  $\text{cm}^3 \text{K mol}^{-1}$  (Er<sup>III</sup>)].<sup>[12]</sup> As the temperature decreases, the  $\chi_M T$  values continuously decrease at 0.1 T.

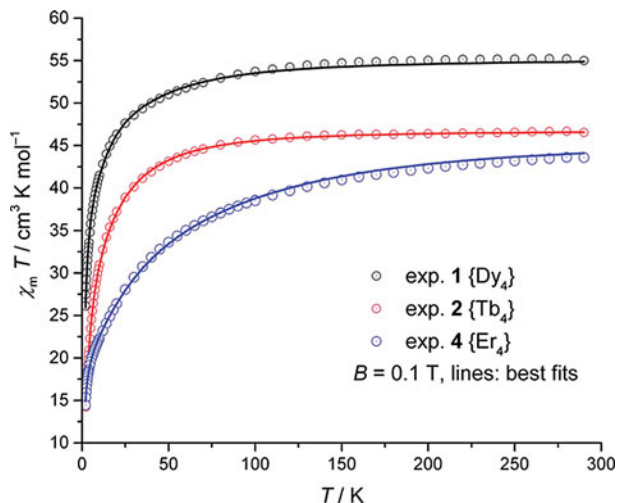


Figure 5. Temperature dependence of  $\chi_M T$  of **1**, **2**, and **4** at  $B = 0.1 \text{ T}$ .

The simple description of the magnetism of **3** is inapplicable for **1**, **2**, and **4** as the ligand field here causes the magnetic susceptibility of each lanthanide center to be anisotropic. The ligand field of each center may be described by a slightly distorted  $D_{2d}$  symmetry (Figure 2): two perpendicular planes each host four ligand atoms (O or N) that form an arc around the lanthanide ion. In a further approximation, the numbers of the considered states of the full basis sets for each cluster (**1**:  $2002^4$ , **2**:  $3003^4$ , **4**:  $364^4$  states) have to be reduced as the amount of available computer memory remains a limiting factor in such calculations. The reduction can be taken care of by implying the combined model:<sup>[14]</sup> the full Hamiltonian including exchange interactions is applied to the ground state (and usually the following excited states). The exchange interactions of a definite number of higher excited states are additionally treated in the molecular-field approximation. Thus, anisotropic exchange interactions and a reduction of the basis sets are taken into account by using this model. On the basis of analyses of the splitting of the energy states in  $D_{2d}$ -symmetric ligand fields, it is sufficient to take eight microstates (related to four Kramer's doublets) for the full Hamiltonian and an additional eight states for the molecular-field approximation, that is, 16 ( $2J + 1$  states of ground multiplet) microstates, for each Dy<sup>III</sup> ion in **1**. In **2** and **4**, the numbers of considered states are  $7 + 6 = 13$  for each Tb<sup>III</sup> ion and  $8 + 8 = 16$  for each Er<sup>III</sup> ion, respectively. In general, these are states of mixed quantum numbers. Owing to the similar structures of **1–4**, the coupling scheme found in **3** has been assumed for all compounds. Although the exchange interaction Hamiltonian is formally the same in all cases, be aware of the decisive difference in the treatment of **3** versus that for **1**, **2** and **4**: although the spin operators represent effective spins for **3**, they represent the true spins for the other compounds and, thus, allow an anisotropic description of the exchange interactions.

The results of the fitting procedures are summarized in Table 3 and depicted as solid lines in Figure 5. As in **3**, all

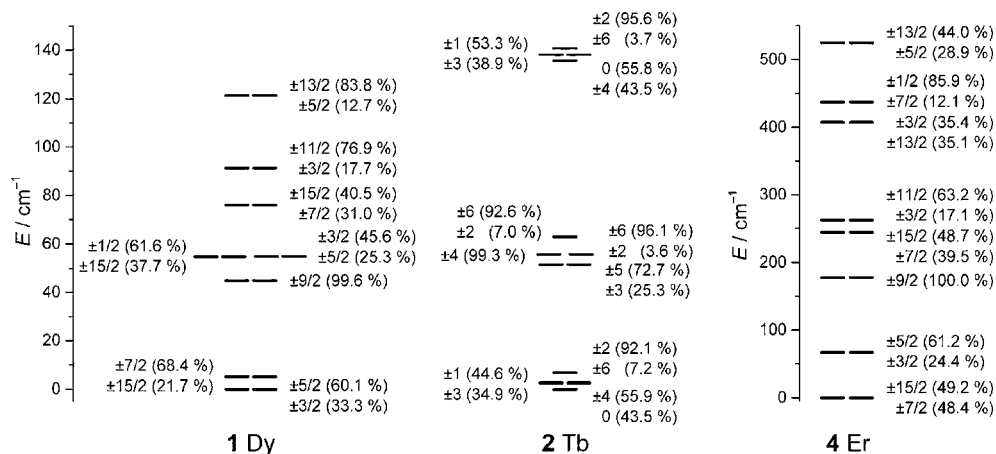


Figure 6. Splitting patterns of the ground multiplets of each lanthanide center (single-ion splitting) in **1**, **2**, and **4**.

exchange interaction parameters  $J_i$  are negative, which reveals that there are weak antiferromagnetic interactions within the  $[2 \times 2]$  square cores of each compound **1–4**. Further, the closer the lanthanide centers are within the cores, the larger the magnitudes of the interactions become. To gain further insight into the meaning of the fitted ligand-field parameters  $B_q^k$  (Wybourne notation) combined with the used spectroscopic parameters, the splittings of the ground multiplets of each individual center of **1**, **2**, and **4** have been calculated and they are shown in Figure 6.

Table 3. Magnetochemical analysis details (all energy values in  $\text{cm}^{-1}$ ) of **1–4**.

|                   | <b>1</b> | <b>2</b> | <b>3</b> | <b>4</b> |
|-------------------|----------|----------|----------|----------|
| $F^2$ [a]         | 94500    | 97650    | –        | 97425    |
| $*F^4$ [a]        | 66320.1  | 68530.8  | –        | 68372.9  |
| $F^6$ [a]         | 50707.0  | 52397.2  | –        | 52276.5  |
| $\zeta_{4f}$ [a]  | 1900     | 1705     | –        | 2393     |
| $B_0^2$           | 78       | 42       | –        | –326     |
| $B_0^4$           | 81       | 45       | –        | 42       |
| $B_4^4$           | –42      | 567      | –        | 238      |
| $B_0^6$           | –356     | –195     | –        | –845     |
| $B_4^6$           | –342     | 130      | –        | –786     |
| $g_{\text{eff}}$  | –        | –        | 1.9925   | –        |
| $J_1$             | –0.14    | –0.30    | –0.11    | –0.18    |
| $J_2$             | –0.03    | –0.04    | –0.06    | –0.11    |
| $J_3$             | –0.01    | –0.02    | –0.03    | –0.04    |
| SQ <sup>[b]</sup> | 0.6%     | 0.4%     | 1.5%     | 0.8%     |

[a] Values are taken from ref.<sup>[15]</sup> and used as constants in the least-squares fitting procedures. [b] The goodness-of-fit parameter SQ is

$$\text{SQ} = \sqrt{\frac{1}{n} \sum_{i=1}^n \frac{(\chi_{\text{exp}}(i) - \chi_{\text{calc}}(i))^2}{\chi_{\text{exp}}^2(i)}}$$

defined as

The calculations show a moderate energy splitting of the Dy and Tb ground states and common levels of Er states. Additionally, the  $M_J$  values (according to Hellwege)<sup>[16]</sup> of each state are given in Figure 6; the (two) largest contributions in the corresponding wave function are shown. The numbers reveal the mixed nature of the states. Note that the centers are weakly coupled and, thus, the states of the whole compounds exhibit mostly states that are centered around these (relative) values.

In addition to the direct current (dc) measurements, alternating current (ac) measurements (3 Oe amplitude) have been performed on **1–4** at zero dc field. No out-of-phase signals have been observed down to 2 K; thus, **1–4** show no single-molecule magnet (SMM) behavior down to this temperature.

## Conclusions

We report the synthesis and structural and magnetic characterization of tetranuclear lanthanide complexes [Ln = Dy (**1**), Tb (**2**), Gd (**3**), and Er (**4**)] that exhibit a  $[2 \times 2]$  square-grid topology. Aroylhydrazone-based Schiff base ligand has been employed to assemble the tetranuclear complexes, and the enol form of the ligand is exclusively utilized. Whereas a simple isotropic model was sufficient to reproduce the temperature- and field-dependent magnetic susceptibility of the Gd analogue, a comprehensive model that takes into account all relevant single-ion effects in addition to the intramolecular nearest-neighbor exchange interactions was necessary to describe the anisotropic derivatives **1**, **2**, and **4**. All of the compounds were found to exhibit weak antiferromagnetic coupling. Also, ac susceptibility measurements down to 2 K at both zero and small dc fields did not reveal any out-of-phase signals characteristic of the slow magnetization relaxation of SMMs.

## Experimental Section

**Reagents and General Procedures:** The solvents and other general reagents used in this work were purified according to standard procedures.<sup>[17]</sup> Pyridine-2,6-dicarboxylic acid, sodium borohydride,  $\text{Dy}(\text{NO}_3)_3 \cdot 5\text{H}_2\text{O}$ ,  $\text{Ho}(\text{NO}_3)_3 \cdot 5\text{H}_2\text{O}$ ,  $\text{Tb}(\text{NO}_3)_3 \cdot 5\text{H}_2\text{O}$ , and  $\text{Gd}(\text{NO}_3)_3 \cdot 6\text{H}_2\text{O}$  were obtained from Sigma–Aldrich and used as received. Hydrazine hydrate (80%), 2-acetylpyridine, and sodium sulfate (anhydrous) were obtained from SD Fine Chemicals, Mumbai, India, and used as received. Methyl-6-(hydroxymethyl)picolinate and 6-(hydroxymethyl)picolinohydrazide<sup>[10]</sup> were prepared according to literature procedures.

**Instrumentation:** The melting points were measured with a JSGW melting point apparatus. The IR spectra were recorded with sam-

ples as KBr pellets with a Bruker Vector 22 FTIR spectrophotometer operating at 400–4000  $\text{cm}^{-1}$ . Elemental analyses of the compounds were obtained with a Thermoquest CE instruments, EA/110 model CHNS-O analyzer. The electrospray ionization mass spectrometry (ESI-MS) spectra were recorded with a Micromass Quattro II triple quadrupole mass spectrometer. The  $^1\text{H}$  NMR spectra were recorded with samples in  $\text{CD}_3\text{OD}$  solutions with a JEOL JNM LAMBDA 400 model spectrometer operating at 400 MHz; chemical shifts are reported in parts per million (ppm) and referenced with respect to internal tetramethylsilane.

**Magnetic Measurements:** The magnetic susceptibility data of **1–4** were obtained with a Quantum Design MPMS-5XL superconducting quantum interference device (SQUID) magnetometer. Polycrystalline samples were compacted and immobilized into cylindrical polytetrafluoroethylene (PTFE) capsules under an Ar atmosphere. The data were acquired as a function of the field and temperature. All data were corrected for the contribution of the sample holder (PTFE capsule), and the diamagnetic contributions of **1–4** were calculated from Pascal's constants (**1**:  $-1.08 \times 10^{-3} \text{ cm}^3 \text{ mol}^{-1}$ , **2**:  $-1.09 \times 10^{-3} \text{ cm}^3 \text{ mol}^{-1}$ , **3**:  $-1.07 \times 10^{-3} \text{ cm}^3 \text{ mol}^{-1}$ , **4**:  $-1.10 \times 10^{-3} \text{ cm}^3 \text{ mol}^{-1}$ ).

**X-ray Crystallography:** The crystal data were collected with a Bruker SMART CCD diffractometer ( $\text{Mo-K}\alpha$  radiation,  $\lambda = 0.71073 \text{ \AA}$ ). The SMART<sup>[18a]</sup> program was used for the collection of frames of data, indexing of reflections, and determination of the lattice parameters, SAINT<sup>[18a]</sup> was used for integration of the intensity of reflections and scaling, SADABS<sup>[18b]</sup> was used for absorption correction, and SHELXTL<sup>[18c,18d]</sup> was used for space-group and structure determination and least-squares refinements on  $F^2$ . All of the structures were solved by direct methods by using the program SHELXS-97<sup>[18e]</sup> and refined by full-matrix least-squares methods against  $F^2$  with SHELXL-97<sup>[18e]</sup>. Hydrogen atoms were fixed at calculated positions, and their positions were refined by a riding model. All non-hydrogen atoms were refined with aniso-

tropic displacement parameters. The crystallographic figures were generated by using the Diamond 3.1e software.<sup>[18f]</sup> The crystal data and the cell parameters for **1–4** are summarized in Table 4.

CCDC-996793 (for **1**), -996794 (for **2**), -996795 (for **3**), and -996796 (for **4**) contain the crystallographic data for this paper. These data can be obtained free of charge from the Cambridge Crystallographic Data Centre via [www.ccdc.cam.ac.uk/data\\_request/cif](http://www.ccdc.cam.ac.uk/data_request/cif).

#### 6-(Hydroxymethyl)-*N'*-[1-(pyridin-2-yl)ethylidene]picolinohydrazide:

An ethanolic solution of 2-acetylpyridine (1.0 mL, 8.97 mmol) was added dropwise to a stirred solution of 6-(hydroxymethyl)picolinohydrazide (1.5 g, 8.97 mmol) in ethanol, and the resulting solution was heated to reflux for 5 h. Then, the solution was allowed to reach room temperature before it was placed in a refrigerator overnight. The white precipitate was collected by filtration, washed successively with cooled methanol and diethyl ether, and finally dried, yield = 1.62 g (66.81%).  $\text{C}_{14}\text{H}_{14}\text{N}_4\text{O}_2$  (270.29): calcd. C 62.21, H 5.22, N 20.73; found C 62.17, H 5.11, N 20.01, m.p. 190, °C.  $^1\text{H}$  NMR ( $\text{CD}_3\text{OD}$ ):  $\delta = 2.55$  (s, 3 H,  $\text{CH}_3$ ), 4.79 (s, 2 H,  $\text{CH}_2$ ), 7.4 (t, 1 H, Py-H), 7.83 (t, 1 H, Py-H), 8.02 (t, 1 H, Py-H), 7.70 (d, 1 H, Py-H), 8.12 (d, 1 H, Py-H), 8.35 (d, 1 H, Py-H), 8.5 (d, 1 H, Py-H) 8.9 (s, NH) ppm. FTIR (KBr):  $\tilde{\nu} = 3314$   $\nu(\text{O-H})$ , 1682  $\nu(\text{C=O})$ , 1597  $\nu(\text{C=N})_{\text{imine}}$ , 1580  $\nu(\text{C=N})_{\text{Py}}$   $\text{cm}^{-1}$ . ESI-MS,  $m/z = 271.11$   $[\text{M} + \text{H}]^+$ .

#### General Procedure for the Synthesis of Homometallic Complexes **1–4**:

A general procedure was employed for the preparation of homometallic complexes **1–4**. To a methanolic solution (40 mL) of  $\text{H}_2\text{L}$ ,  $\text{Ln}(\text{NO}_3)_3 \cdot n\text{H}_2\text{O}$  (For **1**,  $n = 6$ ; **2**,  $n = 5$ ; **3**,  $n = 1$ ; **4**,  $n = 5$ ) was added under stirring. Approximately 15 min later, triethylamine was added dropwise to generate a clear light yellow solution, and the reaction mixture was stirred for 12 h. Then, the resulting solution was concentrated and filtered. Slow diffusion of diethyl ether into the filtrate gave colorless single crystals suitable for X-ray diffraction after one week. Specific details of each reaction and the characterization data of the products are given below.

Table 4. Crystal data and structure refinement parameters of **1–4**.

|   | <b>1</b>   | <b>2</b>   | <b>3</b>  | <b>4</b>   |
|---|--|--|---|--|
| Formula   | $\text{C}_{59}\text{H}_{67}\text{Dy}_4\text{N}_{20}\text{O}_{30}$  | $\text{C}_{59}\text{H}_{74}\text{Tb}_4\text{N}_{20}\text{O}_{30}$  | $\text{C}_{59}\text{H}_{59}\text{Gd}_4\text{N}_{20}\text{O}_{31}$ | $\text{C}_{60}\text{H}_{67}\text{Er}_4\text{N}_{20}\text{O}_{30}$  |
| $M$ / g   | 2186.33  | 2179.11  | 2173.27   | 2217.38  |
| Crystal system                                    | monoclinic   | monoclinic   | monoclinic  | monoclinic   |
| Space group                                       | $P2_1/n$   | $P2_1/n$   | $P2_1/n$  | $P2_1/n$   |
| $a$ / $\text{\AA}$                                | 11.804(5)  | 11.830(6)  | 11.909(4)   | 11.776(5)  |
| $b$ / $\text{\AA}$                                | 23.017(5)  | 22.959(11)   | 22.973(8)   | 22.881(5)  |
| $c$ / $\text{\AA}$                                | 29.117(5)  | 29.140(14)   | 29.131(10)  | 29.049(5)  |
| $\beta$ / °                                       | 90.763(5)  | 90.730(10)   | 91.050(6)   | 90.587(5)  |
| $V$ / $\text{\AA}^3$                              | 7910(4)  | 7915.0(7)  | 7968(5)   | 7827(4)  |
| $Z$   | 4  | 4  | 4   | 4  |
| $\rho_{\text{calcd.}}$ / $\text{g cm}^{-3}$       | 1.836  | 1.829  | 1.811   | 1.882  |
| $\mu$ / $\text{mm}^{-1}$                          | 3.827  | 3.623  | 3.379   | 4.339  |
| $F(000)$  | 4260.0   | 4272.0   | 4228.0  | 4316.0   |
| Crystal size / mm                                 | $0.068 \times 0.043 \times 0.038$                                  | $0.055 \times 0.039 \times 0.021$                                  | $0.059 \times 0.035 \times 0.026$                                 | $0.044 \times 0.031 \times 0.018$                                  |
| $\theta$ range (°)                                | 4.11 to 25.03  | 4.11 to 25.03  | 4.08 to 25.03   | 4.13 to 25.03  |
| Limiting indices                                  | $-10 \leq h \leq 14$ , $-27 \leq k \leq 27$ , $-34 \leq l \leq 29$ | $-12 \leq h \leq 14$ , $-27 \leq k \leq 27$ , $-34 \leq l \leq 32$ | $-14 \leq h \leq 7$ , $-27 \leq k \leq 27$ , $-33 \leq l \leq 34$ | $-14 \leq h \leq 13$ , $-26 \leq k \leq 27$ , $-34 \leq l \leq 28$ |
| Reflections collected                             | 40877  | 53585  | 40664   | 40609  |
| Independent reflections                           | 13902 [ $R(\text{int}) = 0.071$ ]                                  | 13916 [ $R(\text{int}) = 0.046$ ]                                  | 14012 [ $R(\text{int}) = 0.074$ ]                                 | 13724 [ $R(\text{int}) = 0.076$ ]                                  |
| Completeness to $\theta$ (%)                      | 99.5   | 99.5   | 99.4  | 99.4   |
| Data/restraints/parameters                        | 13902/15/995   | 13916/4/1010   | 14012/8/1019  | 13724/33/1014  |
| Goodness-of-fit on $F^2$                          | 1.020  | 1.030  | 0.993   | 1.014  |
| Final $R$ indices [ $I > 2\sigma(I)$ ]            | $R_1 = 0.0595$ , $wR_2 = 0.1475$                                   | $R_1 = 0.0404$ , $wR_2 = 0.0959$                                   | $R_1 = 0.0586$ , $wR_2 = 0.1378$                                  | $R_1 = 0.0606$ , $wR_2 = 0.1476$                                   |
| $R$ indices (all data)                            | $R_1 = 0.0909$ , $wR_2 = 0.1699$                                   | $R_1 = 0.0590$ , $wR_2 = 0.1038$                                   | $R_1 = 0.1133$ , $wR_2 = 0.1702$                                  | $R_1 = 0.0940$ , $wR_2 = 0.1705$                                   |
| Largest diff. peak and hole / $\text{e \AA}^{-3}$ | 2.757 and -1.555   | 1.784 and -1.845   | 1.916 and -1.454  | 3.110 and -2.469   |

[Dy<sub>4</sub>(LH)<sub>4</sub>(μ<sub>2</sub>-OH)<sub>3</sub>(μ<sub>2</sub>-OMe)]||NO<sub>3</sub>||<sub>4</sub>·2MeOH·4H<sub>2</sub>O (**1**): Quantities: Dy(NO<sub>3</sub>)<sub>3</sub>·5H<sub>2</sub>O (0.0649 g, 0.15 mmol), LH<sub>2</sub>(0.04 g, 0.15 mmol), Et<sub>3</sub>N (0.078 mL, 0.6 mmol), yield 0.055 g, 68.75% (based on Dy), m.p. >250 °C. IR (KBr):  $\tilde{\nu}$  = 3426 (b), 3071 (b), 2734 (w), 1611 (s), 1591 (s), 1569 (s), 1540 (s), 1472 (w), 1425 (w), 1369 (s), 1348 (s), 1184 (w), 1162 (w), 1128 (w), 1103 (w), 1035 (w), 1010 (w), 983 (w), 840 (w), 821 (w), 782 (w), 751 (w) cm<sup>-1</sup>. C<sub>59</sub>H<sub>67</sub>Dy<sub>4</sub>N<sub>20</sub>O<sub>30</sub> (2186.33): calcd. C 32.41, H 3.09, N 12.81; found C 32.08, H 3.01, N 12.76.

[Tb<sub>4</sub>(LH)<sub>4</sub>(μ<sub>2</sub>-OH)<sub>3</sub>(μ<sub>2</sub>-OMe)]||NO<sub>3</sub>||<sub>4</sub>·2MeOH·4H<sub>2</sub>O (**2**): Quantities: Tb(NO<sub>3</sub>)<sub>3</sub>·5H<sub>2</sub>O (0.0643 g, 0.15 mmol), LH<sub>2</sub>(0.04 g, 0.15 mmol), Et<sub>3</sub>N (0.078 mL, 0.6 mmol), yield 0.05 g, 62.1% (based on Tb), m.p. >250 °C. IR (KBr):  $\tilde{\nu}$  = 3420 (b), 3071 (b), 2734 (w), 1611 (s), 1591 (s), 1569 (s), 1541 (s), 1475 (w), 1433 (w), 1371 (s), 1350 (s), 1180 (w), 1161 (w), 1132 (w), 1103 (w), 1033 (w), 1007 (w), 981 (w), 849 (w), 821 (w), 775 (w), 757 (w) cm<sup>-1</sup>. C<sub>59</sub>H<sub>74</sub>N<sub>20</sub>O<sub>30</sub>Tb<sub>4</sub> (2179.11): calcd. C 32.52, H 3.42, N 12.86; found C 32.01, H 3.39, N 12.71.

[Gd<sub>4</sub>(LH)<sub>4</sub>(μ<sub>2</sub>-OH)<sub>3</sub>(μ<sub>2</sub>-OMe)]||NO<sub>3</sub>||<sub>4</sub>·2MeOH·5H<sub>2</sub>O (**3**): Quantities: Gd(NO<sub>3</sub>)<sub>3</sub>·6H<sub>2</sub>O (0.067 g, 0.15 mmol), LH<sub>2</sub>(0.04 g, 0.15 mmol), Et<sub>3</sub>N (0.078 mL, 0.6 mmol), yield 0.052 g, 64.47% (based on Gd), m.p. >250 °C. IR (KBr):  $\tilde{\nu}$  = 3424 (b), 3072 (b), 2734 (w), 1611 (s), 1591 (s), 1572 (s), 1543 (s), 1472 (w), 1429 (w), 1371 (s), 1350 (s), 1185 (w), 1162 (w), 1132 (w), 1103 (w), 1035 (w), 1010 (w), 987 (w), 849 (w), 821 (w), 782 (w), 757 (w) cm<sup>-1</sup>. C<sub>59</sub>H<sub>59</sub>Gd<sub>4</sub>N<sub>20</sub>O<sub>31</sub> (2173.27): calcd. C 32.61, H 2.74, N 12.89; found C 32.50, H 3.27, N 12.53.

[Er<sub>4</sub>(LH)<sub>4</sub>(μ<sub>2</sub>-OH)<sub>3</sub>(μ<sub>2</sub>-OMe)]||NO<sub>3</sub>||<sub>4</sub>·3MeOH·3H<sub>2</sub>O (**4**): Quantities: Er(NO<sub>3</sub>)<sub>3</sub>·5H<sub>2</sub>O (0.066 g, 0.15 mmol), LH<sub>2</sub>(0.04 g, 0.15 mmol), Et<sub>3</sub>N (0.078 mL, 0.6 mmol), yield 0.058 g, 70.3% (based on Er), m.p. >250 °C. IR (KBr):  $\tilde{\nu}$  = 3424 (b), 3072 (b), 2734 (w), 1610 (s), 1589 (s), 1572 (s), 1538 (s), 1465 (w), 1426 (w), 1371 (s), 1350 (s), 1185 (w), 1160 (w), 1132 (w), 1103 (w), 1038 (w), 1015 (w), 987 (w), 845 (w), 831 (w), 789 (w), 756 (w) cm<sup>-1</sup>. C<sub>60</sub>H<sub>67</sub>Er<sub>4</sub>N<sub>20</sub>O<sub>30</sub> (2217.38): calcd. C 32.50, H 3.05, N 12.63; found C 32.39, H 3.18, N 12.50.

**Supporting Information** (see footnote on the first page of this article): Literature-reported topologies of tetranuclear lanthanide complexes, molecular structures of **1**, **3**, and **4**, and list of bond lengths and angles.

## Acknowledgments

The authors are thankful to the Department of Science and Technology (DST), New Delhi for financial support. S. B. and S. D. thank the Council of Scientific and Industrial Research (CSIR), India for Senior Research Fellowships. V. C. is thankful to the Department of Science and Technology for a J. C. Bose National Fellowship.

- [1] a) P. W. Roesky, G. C.-Melchor, A. Zulys, *Chem. Commun.* **2004**, 738; b) X. Yu, S. Y. Seo, M. J. Tobin, *J. Am. Chem. Soc.* **2007**, *129*, 7244; c) T. N. Parac-Vogt, K. Deleersnyder, K. Binnemans, *Eur. J. Org. Chem.* **2005**, 1810; d) F. Pohki, S. Doye, *Chem. Soc. Rev.* **2003**, *32*, 104; e) P. W. Roesky, T. E. Müller, *Angew. Chem. Int. Ed.* **2003**, *42*, 2708; *Angew. Chem.* **2003**, *115*, 2812.
- [2] a) M. Romanelli, G. A. Kumar, T. J. Emge, R. E. Riman, J. G. Brennan, *Angew. Chem. Int. Ed.* **2008**, *47*, 6049; *Angew. Chem.* **2008**, *120*, 6138; b) C. M. G. dos Santos, A. J. Harte, S. J. Quinn, T. Gunnlaugsson, *Coord. Chem. Rev.* **2008**, *252*, 2512; c) S. Faulkner, L. Natrajan, S. William, D. Sykes, *Dalton Trans.* **2009**, 3890; d) K. Binnemans, *Coord. Chem. Rev.* **2009**, *109*, 4283; e) M. D. Ward, *Coord. Chem. Rev.* **2007**, *251*, 1663; f) S. Sivakumar, M. L. P. Reddy, *J. Mater. Chem.* **2012**, *22*, 10852.
- [3] a) D. Gatteschi, A. Caneschi, L. Pardi, R. Sessoli, *Science* **1994**, *265*, 1054; b) R. Sessoli, L. H. Tsai, R. A. Schake, S. Wang, B. J. Vincent, K. Folting, D. Gatteschi, G. Christou, N. D. Hendrickson, *J. Am. Chem. Soc.* **1993**, *115*, 1804; c) A. Yamashita, A. Watanabe, S. Akine, T. Nabeshima, M. Nakano, T. Yamamura, T. Kajiwara, *Angew. Chem. Int. Ed.* **2011**, *50*, 4016; *Angew. Chem.* **2011**, *123*, 4102; d) E. Colacio, J. Ruiz, A. J. Mota, M. A. Palacios, E. Cremades, E. Ruiz, F. J. White, E. K. Brechin, *Inorg. Chem.* **2012**, *51*, 5857; e) F. Tuna, C. A. Smith, M. Bodensteiner, L. Ungur, L. F. Chibotaru, E. J. L. McInnes, R. E. P. Winpenny, D. Collison, R. A. Layfield, *Angew. Chem. Int. Ed.* **2012**, *51*, 6976; *Angew. Chem.* **2012**, *124*, 7082; f) V. Mereacre, *Angew. Chem. Int. Ed.* **2012**, *51*, 9922; *Angew. Chem.* **2012**, *124*, 10060; g) J. Goura, J. P. S. Walsh, F. Tuna, V. Chandrasekhar, *Inorg. Chem.* **2014**, *53*, 3385; h) S. Das, A. Dey, S. Biswas, E. Colacio, V. Chandrasekhar, *Inorg. Chem.* **2014**, *53*, 3417; i) V. E. Campbell, H. Bolvin, E. Rivière, R. Guillot, W. Wernsdorfer, T. Mallah, *Inorg. Chem.* **2014**, *53*, 2598.
- [4] a) A. Picot, A. D'Aléo, P. L. Baldeck, A. Grichine, A. Duperray, C. Andraud, O. Maury, *J. Am. Chem. Soc.* **2008**, *130*, 1532; b) M. Bottrill, L. Kwok, N. Long, *Chem. Soc. Rev.* **2006**, *35*, 557.
- [5] a) J. J. Baldoví, S. C.-Serra, J. M. Clemente-Juan, E. Coronado, A. G.-Ariño, A. Palií, *Inorg. Chem.* **2012**, *51*, 12565; b) P. H. Lin, T. J. Burchell, R. Clerac, M. Murugesu, *Angew. Chem. Int. Ed.* **2008**, *47*, 8848; *Angew. Chem.* **2008**, *120*, 8980; c) M. T. Gamer, Y. Lan, P. W. Roesky, A. K. Powell, R. Clerac, *Inorg. Chem.* **2008**, *47*, 6581; d) B. Hussain, D. Savard, T. J. Burchell, W. Wernsdorfer, M. Murugesu, *Chem. Commun.* **2009**, 1100; e) X.-J. Zheng, L.-P. Jin, S. Gao, *Inorg. Chem.* **2004**, *43*, 1600; f) T. Kajiwara, H. Wu, T. Ito, N. Iki, S. Miyano, *Angew. Chem. Int. Ed.* **2004**, *43*, 1832; *Angew. Chem.* **2004**, *116*, 1868; g) G.-F. Xu, P. Gamez, S. J. Teat, J. Tang, *Dalton Trans.* **2010**, *39*, 4353; h) L. G. Westin, M. Kritikos, A. Caneschi, *Chem. Commun.* **2003**, 1012; i) P. C. Andrews, T. Beck, C. M. Forsyth, B. H. Fraser, P. C. Junk, M. Massi, P. W. Roesky, *Dalton Trans.* **2007**, 5651; j) A. S. R. Chesman, D. R. Turner, B. Moubaraki, K. S. Murray, G. B. Deacon, S. R. Batten, *Chem. Eur. J.* **2009**, *15*, 5203; k) R. Wang, D. Song, S. Wang, *Chem. Commun.* **2002**, 368; l) R. Wang, Z. Zheng, T. Jin, R. J. Staples, *Angew. Chem. Int. Ed.* **1999**, *38*, 1813; *Angew. Chem.* **1999**, *111*, 1929; m) X. Gu, D. Xue, *Inorg. Chem.* **2007**, *46*, 3212; n) X.-J. Kong, Y. Wu, L.-S. Long, L.-S. Zheng, Z. Zheng, *J. Am. Chem. Soc.* **2009**, *131*, 6918.
- [6] S. Xue, L. Zhao, Y.-N. Guo, J. Tang, *Dalton Trans.* **2012**, *41*, 351.
- [7] N. M. Randell, M. U. Anwar, M. W. Drover, L. N. Dawe, L. K. Thompson, *Inorg. Chem.* **2013**, *52*, 6731.
- [8] M. U. Anwar, L. K. Thompson, L. N. Dawe, F. Habib, M. Murugesu, *Chem. Commun.* **2012**, *48*, 4576.
- [9] V. Chandrasekhar, S. Hossain, S. Das, S. Biswas, J.-P. Sutter, *Inorg. Chem.* **2013**, *52*, 6346.
- [10] V. Chandrasekhar, S. Das, A. Dey, S. Hossain, J.-P. Sutter, *Inorg. Chem.* **2013**, *52*, 11956.
- [11] M. Speldrich, H. Schilder, H. Lueken, P. Kögerler, *Isr. J. Chem.* **2011**, *51*, 215; see also <http://www.condon.fh-aachen.de/>.
- [12] H. Lueken, *Magnetochemie*, Teubner, Stuttgart, Germany, **1999**.
- [13] B. Wang, S. Jiang, X. Wang, S. Gaom, *Lanthanide Based Magnetic Molecular Materials*, in: *Rare Earth Coordination Chemistry: Fundamentals and Applications* (Ed.: C. Huang), Wiley, Chichester, UK, **2010**, and references cited therein.
- [14] a) M. E. Lines, *J. Chem. Phys.* **1971**, *55*, 2977; b) H. Lueken, P. Hannibal, K. Handrick, J. Schmitz, *Z. Kristallogr.* **1989**, *186*, 185.

- [15] J. S. Griffith, *The Theory of Transition-Metal Ions*, Cambridge University Press, Cambridge, **1961**.
- [16] K. H. Hellwege, *Ann. Phys.* **1948**, 439, 95.
- [17] B. S. Furniss, A. J. Hannaford, P. W. G. Smith, Tatchell, A. R. *Vogel's Textbook of Practical Organic Chemistry*, 5th ed., ELBS, Longman, London, **1989**.
- [18] a) *SMART & SAINT Software Reference Manuals*, v. 6.45, Bruker Analytical X-ray Systems, Inc., Madison, **2003**; b) G. M. Sheldrick, *SADABS, Software for Empirical Absorption Correction*, v. 2.05, University of Göttingen, Germany, **2002**; c) *SHELXTL Reference Manual*, ver. 6.1, Bruker Analytical X-ray Systems, Madison, **2000**; d) G. M. Sheldrick, *SHELXTL*, v. 6.12, Bruker AXS Inc., Madison, **2001**; e) G. M. Sheldrick, *SHELXL97, Program for Crystal Structure Refinement*, University of Göttingen, Germany, **1997**; f) K. Bradenburg, *Diamond*, v. 3.1eM, Crystal Impact, Bonn, Germany, **2005**.

Received: April 17, 2014

Published Online: ■

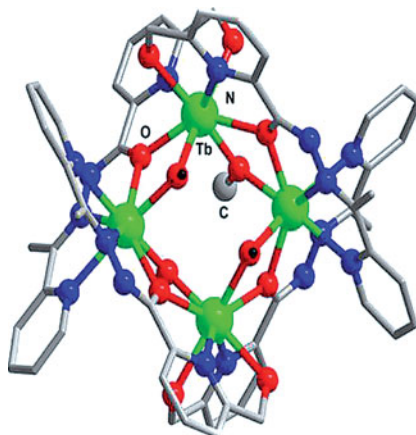
## Lanthanide Complexes

S. Biswas, S. Das, J. van Leusen,  
P. Kögerler,\* V. Chandrasekhar\* ..... 1–10



Tetranuclear [2×2] Square-Grid Lanthanide(III) Complexes: Syntheses, Structures, and Magnetic Properties

**Keywords:** Lanthanides / Cluster compounds / Schiff bases / Magnetic properties



The reactions of a multicompartamental ligand with rare-earth(III) nitrate salts afford a series of homometallic Ln<sub>4</sub> complexes [Ln = Dy, Tb, Gd, and Er] with [2×2] square-grid topology. Magnetic studies reveal the presence of all-antiferromagnetic exchange interactions and ligand-field-induced effects for the Dy, Tb, and Er complexes, whereas an isotropic model suffices for the Gd complex.